Inorg. Chem. **2005**, *44*, 8836–8845

Pillared-Layer Microporous Metal–Organic Frameworks Constructed by Robust Hydrogen Bonds. Synthesis, Characterization, and Magnetic and Adsorption Properties of 2,2′-Biimidazole and Carboxylate Complexes

Bing-Bing Ding, Yan-Qin Weng, Zong-Wan Mao, Chi-Keung Lam, Xiao-Ming Chen, and Bao-Hui Ye*

School of Chemistry and Chemical Engineering, Sun Yat-Sen University, Guangzhou 510275, China

Received July 18, 2005

Two new isostructural complexes $[M(H_2biim)_3][M(btc)(Hbiim)]\cdot 2H_2O$ (M = Co, (**1**); M = Ni, (**2**)) (btc = 1,3,5-benzenetricarboxylate; H_2biim = 2,2′-biimidazole) have been synthesized and characterized by single-crystal X-ray diffraction. They present a unique structure consisting of two distinct units: the monomeric cations $[M(H_2biim)_3]^{2+}$ and the two-dimensional (2D) anionic polymer $[M(Hbiim)(btc)]^{2-}$. In the anionic moiety, the $Hbiim^-$ monoanion is simultaneously coordinated to one metal atom in a bidentate mode and further to another metal atom in a monodentate mode. The imidazolate groups bridge the two adjacent metal ions into a helical chain which is further arranged in left- and right-handed manners. These chains are bridged by btc ligands into a 2D brick wall structure. The most interesting aspect is that the $[M(H_2biim)_3]^{2+}$ cations act as pillars and link the anionic layers via robust heteromeric hydrogen-bonded synthons $R_2^2(9)$ and $R_2^1(7)$ formed by the uncoordinated oxygen atoms of carboxylate groups and the H_2biim ligands, resulting in a microporous metal–organic framework with one-dimensional (1D) channels (ca. 11.85 Å × 11.85 Å for **1** and 11.43 Å × 11.43 Å for **2**). Magnetic properties of these two complexes have also been studied in the temperature range of 2–300 K, and their magnetic susceptibilities obey the Curie–Weiss law in the temperature range of 20–300 K (for **1**) and 2–300 K (for **2**), respectively, showing anti-ferromagnetic coupling through imidazolate bridging. Taking into consideration the Heisenberg infinite chain model as well as the possibility of chain-to-chain and chain-to-cation interactions, the anti-ferromagnetic exchange of **2** is analyzed via a correction for the molecular field, giving the values of $g_{cat} = 2.296$, $g_{Ni} = 2.564$, $J = -13.30$ cm^{-1}, and $zJ' = -0.017$ cm^{-1}. The microporous frameworks are stable at ca. 350 °C. They do not collapse after removal of the guest water molecules in the channels, and they adsorb methanol molecules selectively.

Introduction

Metal−organic frameworks (MOFs) are considered to be promising materials for many applications, such as catalysis, separation, gas storage, sensing, magnetism, and ion exchange.[1] Compared to the classically microporous inorganic materials such as zeolites, structures of MOFs are easy controlled and the pores can be functionalized through modification of the walls. However, rational design and synthesis of MOFs with unique structure and function is still hard work. Therefore, the development of rational synthetic methods for the design of the architecture of structurally well-defined solids is the most significant point for MOFs. The pillared-layer assemblies have been proven to be an effective and controllable route to produce three-dimensional (3D) networks with functionalized channels or pores for selective absorption of gases or solvents through modification of the pillar module in the interlamellar region.[2] Although the

* To whom correspondence should be addressed. Fax: (86)-20-84112245. Tel.: (86)-20-84113986. E-mail: cesybh@zsu.edu.cn.

(1) (a) Seo, J. S.; Whang, D.; Lee, H.; Jun, S. I.; Oh, J.; Jeon, Y.; Kim, K. *Nature* **2000**, *404*, 982. (b) Halder, G., J.; Kepert, C. J.; Moubaraki, B.; Murray, K. S.; Cashion, J. D. *Science* **2002**, *298*, 1762. (c) Eddaoudi, M.; Kim, J.; Rosi, N. L.; Vodak, D.; Wachter, J.; O'Keeffe, M.; Yaghi, O. M. *Science* **2002**, *295*, 469. (d) Rosi, N. L.; Eckert, J.; Eddaoudi, M.; Vodak, D. T.; Kim, J.; O'Keeffe, M.; Yaghi, O. M. *Science* **2003**, *300*, 1127. (e) Takamizawa, S.; Nakata, E.; Yokoyama, H.; Mochizuki, K.; Mori, W. *Angew. Chem., Int. Ed.* **2003**, *42*, 4331. (f) Dybtsev, D. N.; Chun, H.; Yoon, S. H.; Kim, D.; Kim, K. *J. Am. Chem. Soc.* **2004**, *126*, 32. (g) Kitagawa, S.; Kitaura, R.; Noro, S.-I. *Angew. Chem., Int. Ed.* **2004**, *43*, 2334. (h) Snurr, R. Q.; Hupp, J. T.; Nguyen, S. T. *AIChE J.* **2004**, *50*, 1090. (i) Pan, L.; Sander, M. B.; Huang, X.; Li, J.; Smith, M.; Bittner, E.; Bockrath, B.; Johnson, J. K. *J. Am. Chem. Soc.* **2004**, *126*, 1308. (j) Kesanli, B.; Cui, Y.; Smith, M. R.; Bittner, E. W.; Bockrath, B. C.; Lin, W.-B. *Angew. Chem., Int. Ed.* **2005**, *44*, 72.

(2) (a) Kitagawa, S.; Uemura, K. *Chem. Soc. Rev.* **2005**, *34*, 109. (b) Kitaura, R.; Kitagawa, S.; Kubota, Y.; Kobayashi, T. C.; Kindo, K.; Mita, Y.; Matsuo, A.; Kobayashi, M.; Chang, H. C.; Ozawa, T. C.; Suzuki, M.; Sakata, M.; Takata, M. *Science* **2002**, *298*, 2358.

10.1021/ic051195k CCC: $30.25
Published on Web 10/14/2005

pillared-layer 3D networks constructed via coordination bonding, in which organic ligands,[3] simple inorganic anoins,[4] or polyoxometalates[5] generally act as pillars, have been well documented,[2] the coordinated cations or anions functioning as pillars that further link the layers into a 3D framework via hydrogen bonding have not been reported so far.[2]

The use of coordinative unsaturated ligands in controlling the supramolecular architecture of transition metal complexes via coordination or hydrogen bonding may lead to the formation of oligomers, polymers, or porous frameworks possessing unusual structures and fascinating properties.[6] The metal complexes of imidazolate and its derivatives have been widely used in this area because the nitrogen atom of imidazole can be deprotonated at a high pH value and can further bind the other metal ion into oligomers or higher dimensional frameworks.[7−17] These observations show that the imidazolate linkage with a π-delocalized nature promotes magnetic exchange between paramagnetic metal centers.[7h,9c,9f] In our quest for new ligands for the construction of polymetallic systems with novel structural features, we found that metallic complexes of 2,2′-biimidazole (H_2biim) and its derivatives are good candidates because the H_2biim ligand possesses two important features. First, the imino moieties can be coordinated to metal ions and the amino groups may act as a donor in hydrogen bonding interactions. Second, the H_2biim can serve as a neutral bidentate (H_2biim), a tridentate ($Hbiim^-$), or a tetradentate ($biim^{2-}$) ligand, depending on its protonation state. The transition metal complexes of the neutral ligand H_2biim[18−27] have been found

(3) (a) Kitaura, R.; Fujimoto, K.; Noro, S.; Kondo, M,; Kitagawa, S. *Angew. Chem., Int. Ed.* **2002**, *41*, 133. (b) Maji, T. K.; Uemura, K.; Chang, H. C.; Matsuda, R.; Kitagawa, S. *Angew. Chem., Int. Ed*. **2004**, *43*, 3269. (c) Hung, L.; Wang, S. L.; Kao, H. M.; Lii, K. H. *Inorg. Chem*. **2002**, *41*, 3929. (d) Wang, C. M.; Lii, K. H. *J. Solid State Chem*. **2003**, *172*, 194. (e) Chang, W. K.; Chiang, R. K.; Jiang, Y. C.; Wang. S. L.; Lee, S. F.; Lii, K. H. *Inorg. Chem*. **2004**, *43*, 2564. (f) Lin, Z. E.; Zhang, J.; Zheng, S. T.; Yang, G. Y. *Microporous Mesoporous Mater*. **2004**, *68*, 65. (g) Yu, T.; Tian, Y. Q.; Chen, Z. X.; Chen, J. X.; Weng, L. H.; Zhao, D. Y. *Chem. Lett*. **2004**, 1514. (h) Chun, H.; Dyunuk, D.; Kim, K. *Chem.—Eur. J*. **2005**, *11*, 3521.

(4) Chakrabarti, S.; Natarajian, S. *J. Chem. Soc., Dalton Trans*. **2002**, 4156.

(5) Lü, J.; Shen, E.-H.; Li, Y.-G.; Xiao, D.-G.; Wang, E.-B.; Xu, L. *Cryst. Growth Des.* **2005**, *5*, 65.

(6) (a) Chen, B.; Eddaoudi, M.; Reineke, T. M.; Kampf, J. W.; O'Keeffe, M.; Yaghi, O. M. *J. Am. Chem. Soc*. **2000**, *122*, 11559. (b) Goldberg, I. *Chem.—Eur. J*. **2000**, *6*, 3863. (c) Su, C.-Y.; Cai, Y.-P.; Chen, C.-L.; Kang, B.-S. *Inorg. Chem.* **2001**, *40*, 2210. (d) Pal, I.; Basuli, F.; Mak, T. C. W.; Bhattacharya, S. *Angew. Chem., Int. Ed.* **2001**, *40*, 2923. (e) Winpenny, R. E. P. *J. Chem. Soc., Dalton Trans.* **2002**, 1. (f) Campagna, S.; Pietro, C. D.; Loiseau, F.; Maubert, B.; McClenaghan, N.; Passalacqna, R.; Puntoriero, F.; Ricevuto, V.; Serroni, S. *Coord. Chem. Rev.* **2002**, *229*, 67. (g) Kosal, M. E.; Chou, J.-H.; Wilson, S. R.; Suslick, K. S. *Nat. Mater*. **2002**, *1*, 118. (h) Smithenry, D. W.; Wilson, S. R.; Suslick, K. S. *Inorg. Chem*. **2003**, *42*, 7719. (i) Lin, X.; Doble, D. M. J.; Blake, A. J.; Harrison, A.; Wilson, C.; Schröder, M. *J. Am. Chem. Soc.* **2003**, *125*, 9476. (j) Kitaura, R.; Onoyama, G.; Sakamoto, H.; Matsuda, R.; Noro, S.; Kitagawa, S. *Angew. Chem., Int. Ed.* **2004**, *43*, 2684.

(7) For Co: (a) Sturm, M.; Brandl, F.; Engel, D.; Hoppe, W. *Acta Crystallogr., Sect. B* **1975**, *31*, 2369. (b) Hawkins, C. J.; Horn, E.; Martin, J.; Palmer, J. A. L.; Snow, M. R. *Aust. J. Chem.* **1986**, *39*, 1213. (c) Brown, S. J.; Olmstead, M. M.; Mascharak, P. K. *Inorg. Chem.* **1989**, *28*, 3720. (d) Blackman, A. G.; Buckingham, D. A.; Clark, C. R.; Simpson, J. *J. Chem. Soc., Dalton Trans.* **1991**, 3031. (e) Yamanari, K.; Fukuda, I.; Kawamoto, T.; Kushi, Y.; Fuyuhiro, A.; Kubota, N.; Fukuo, T.; Arakawa, R. *Inorg. Chem.* **1998**, *37*, 5611. (f) Moore, S. J.; Kutikov, A.; Lachicotte, R. J.; Marzilli, L. G. *Inorg. Chem.* **1999**, *38*, 768. (g) Katsuki, I.; Motoda, Y.; Sunatski, Y.; Matsumoto, N.; Nakashima, T.; Kojima, M. *J. Am. Chem. Soc.* **2002**, *124*, 629. (h) Tian, Y.-Q.; Cai, C.-X.; Ji, Y.; You, X.-Z.; Peng, S.-M.; Lee, G.-H. *Angew. Chem., Int. Ed.* **2002**, *41*, 1384. (i) Tian, Y.-Q.; Cai, C.-X.; Ren, X.-M.; Duan, C.-Y.; Xu, Y.; Gao, S.; You, X.-Z. *Chem.—Eur. J.* **2003**, *9*, 5673.

(8) For Ni: (a) Thanyasiri, T.; Sinn, E. *J. Chem. Soc., Dalton Trans.* **1989**, 1187. (b) Costes, J.-P.; Dahan, F.; Laurent, J.-P. *Inorg. Chem.* **1991**, *30*, 1887. (c) Hu, H.-M.; Sun, H.-S.; Zhao, Q.; Yu, Z.; Huang, X.-Y.; You, X.-Z. *J. Coord. Chem.* **1998**, *43*, 361. (d) Mimura, M.; Matsuo, T.; Matsumoto, N.; Takamizawa, S.; Mori, W.; Re, N. *Bull. Chem. Soc. Jpn.* **1998**, *71*, 1831. (e) Niu, S.-Y.; Jin, J.; Yang, Z.-Z.; Yang, G.-D.; Ye, L. *J. Mol. Struct.* **2002**, *643*, 123. (f) Masciocchi, N.; Castelli, F.; Forster, P. M.; Tafoya, M. M.; Cheetham, A. K. *Inorg. Chem.* **2003**, *42*, 6147.

(9) For Fe: (a) Lehnert, R.; Seel, F. *Z. Anorg. Allg. Chem.* **1978**, *444*, 91. (b) Spek, A. L.; Duisenberg, A. J. M.; Feiters, M. C. *Acta Crystallogr., Sect. C* **1983**, *39*, 1212. (c) Rettig, S. J.; Storr, A.; Summers, D. A.; Thompson, R. C.; Trotter, J. *J. Am. Chem. Soc.* **1997**, *119*, 8675. (d) Rettig, S. J.; Storr, A.; Summers, D. A.; Thompson, R. C.; Trotter, J. *Can. J. Chem.* **1999**, *77*, 425. (e) Lambert, F.; Policar, C.; Durot, S.; Cesario, M.; Lu, Y.; Korri-Youssoufi, H.; Keita, B.; Nadjo, L. *Inorg. Chem*. **2004**, *43*, 4178. (f) Sunatsuki, Y.; Ohta, H.; Kojima, M.; Ikuta, Y.; Goto, Y.; Matsumoto, N.; Iijima, S.; Akashi, H.; Kaizaki, S.; Dahan, F.; Tuchagues, J.-P. *Inorg. Chem*. **2004**, *43*, 4154.

(10) For Cu: (a) Ivarsson, G.; Lundberg, B. K. S.; Ingri, N. *Acta Chem. Scand.* **1972**, *26*, 3005. (b) Lundberg, B. K. S. *Acta Chem. Scand.* **1972**, *26*, 3902. (c) Koolhaas, G. J. A. A.; Driessen, W. L.; Van Koningsbruggen, P. J.; Reedijk, J.; Spek, A. L. *J. Chem. Soc., Dalton Trans.* **1993**, 3803. (d) Matsumoto, N.; Nozaki, T.; Ushio, H.; Motada, K.; Ohba, M.; Mago, G.; Okawa, H. *J. Chem. Soc., Dalton Trans.* **1993**, 2157. (e) Matsumoto, N.; Mizuguchi, Y.; Magao, G.; Eguchi, S.; Miyasaka, H.; Nakashimha, T.; Tuchagues, J.-P. *Angew. Chem., Int. Ed. Engl*. **1997**, *36*, 1860. (f) Miyasaka, H.; Okamura, S.; Nakashima, T.; Matsumoto, N. *Inorg. Chem*. **1997**, *36*, 4329. (g) Shii, Y.; Motoda, Y.; Matsuo, T.; Kai, F.; Nakashima, T.; Tuchagues, J.-P.; Matsumoto, N. *Inorg. Chem.* **1999**, *38*, 3513. (h) Matsumoto, N.; Motoda, Y.; Matsuo, T.; Nakashima, T.; Re, N.; Dahan, F.; Tuchagues, J.-P. *Inorg. Chem.* **1999**, *38*, 1165. (i) Masciocchi, N.; Bruni, S.; Cariati, E.; Cariati, F.; Galli, S.; Sironi, A. *Inorg. Chem.* **2001**, *40*, 5897. (j) Song, Y.; Gamez, P.; Stassen, A. F.; Lutz, M.; Spek, A. L.; Reedijk, J. *Eur. J. Inorg. Chem.* **2003**, 4073. (k) Huang, X.-C.; Zhang, J.-P.; Lin, Y.-Y.; Yu, X.-L.; Chen, X.-M. *Chem. Commun*. **2004**, 1100. (l) Huang, X.-C.; Zhang, J.-P. Chen, X.-M. *J. Am. Chem. Soc*. **2004**, *126*, 13218. (m) Huang, X.-C.; Zhang, J.-P.; Lin, Y.-Y.; Yu, X.-L.; Chen, X.-M. *Chem. Commun*. **2005**, 2232.

(11) For Mn: Lehnert, R.; Seel, F. *Z. Anorg. Allg. Chem.* **1980**, *464*, 187.

(12) For Zn: (a) Ashby, C. I. H.; Cheng, C. P.; Duesler, E. N.; Brown, T. L. *J. Am. Chem. Soc.* **1978**, *100*, 6063. (b) Huang, X.-C.; Li, D.; Tong, Y.-X.; Chen, X.-M. *Acta Sci. Nat. Univ. Sunyatseni* **1998**, *37*, 55. (c) Huang, X.-C.; Zahng, J.-P.; Chen, X.-M. *Chin. Sci. Bull.* **2003**, *48*, 1531.

(13) For Ag: Masciocchi, N.; Moret, M.; Cairati, P.; Sironi, A.; Ardizzoia, G. A.; La Monica, G. *J. Chem. Soc., Dalton Trans.* **1995**, 1671.

(14) For Hg and Cd: Masciocchi, N.; Ardizzoia, G. A.; Brenna, S.; Castelli, F.; Galli, S.; Maspero, A.; Sironi, A. *Chem. Commun.* **2003**, 2018.

(15) For Rh: Lehaire, M.-L.; Scopelliti, R.; Herdeis, L.; Polborn, K.; Mayer, P.; Severin, K. *Inorg. Chem.* **2004**, *43*, 1609.

(16) For Pd: Miyasaka, H.; Nakashimha, T.; Tuchagues, J.-P. *Angew. Chem., Int. Ed. Engl*. **1997**, *36*, 1860.

(17) For Au: Wienken, M.; Lippert, B.; Zangrando, E.; Randaccio, L. *Inorg. Chem*. **1992**, *31*, 1983.

(18) (a) Dance, I. G.; Abushamleh, A. S.; Goodwin, H. A. *Inorg. Chim. Acta* **1980**, *43*, 217. (b) Boinnard, D.; Cassoux, P.; Petrouleas, V.; Savariault, J.-M.; Tuchagues, J.-P. *Inorg. Chem.* **1990**, *29*, 4114. (c) Matouzenko, G. S.; Letard, J.-F.; Lecocq, S.; Bousseksou, A.; Capes, L.; Salmon, L.; Perrin, M.; Kahn, O.; Collet, A. *Eur. J. Inorg. Chem.* **2001**, 2935.

(19) (a) Mighell, A. D.; Reimann, C. W.; Mauer, F. A. *Acta Crystallogr., Sect. B* **1969**, *25*, 60. (b) van Albada, G. A.; Mohamadou, A.; Mutikainen, I.; Turpeinen, U.; Reedijk, J. *Acta Crystallogr., Sect. E* **2004**, *60*, m237.

(20) (a) Bencini, A.; Mani, F. *Inorg. Chim. Acta* **1988**, *154*, 215. (b) Haj, M. A.; Quiros, M.; Salas, J. M.; Dobado, J. A.; Molina, J. M.; Basallote, M. G.; Manez, M. A. *Eur. J. Inorg. Chem.* **2002**, 811. (c) Mohamadou, A.; van Albada, G. A.; Kooijman, H.; Wieczorek, B.; Spek, A. L.; Reedijk, J. *New J. Chem.* **2003**, *27*, 983.

(21) Kirchner, C.; Krebs, B. *Inorg. Chem.* **1987**, *26*, 3569.

(22) Marshall, S. R.; Incarvito, C. D.; Shum, W. W.; Rheingold, A. L.; Miller, J. S. *Chem. Commun.* **2002**, 3006.

Scheme 1. Schematic Representation of the Possible Connection Modes for Metal 2,2′-Biimidazole Complexes

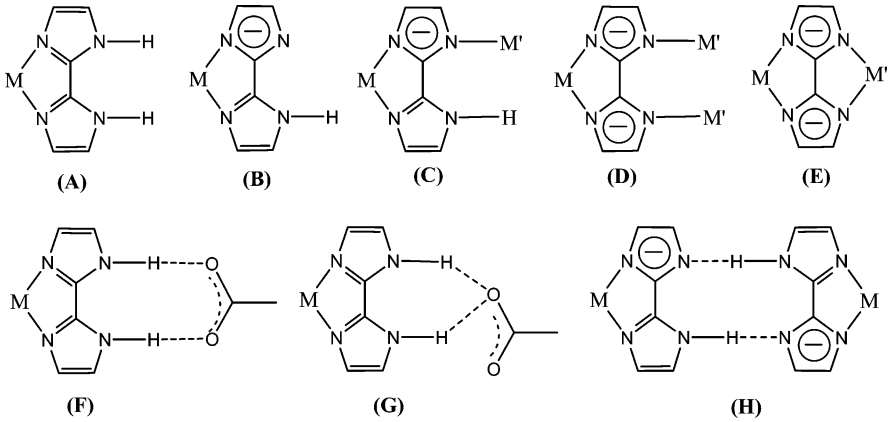

to be coordinated in type-A mode (Scheme 1). Interestingly, fragment A can be further interacted with carboxylate groups via hydrogen bonds to assemble into multidimensional structures. In this case, one or two oxygen atom(s) of a carboxylate group can join directly to the N−H donors via a charge-assisted heteromeric hydrogen-bonded synthon of $R_2^2(9)$ or $R_2^1(7)$,[28] as depicted in types F and G.[29] In the monoanion Hbiim$^-$ mode (type B), the H_2biim ligand is partially deprotonated. Fragment B has been used to produce extended inorganic supramolecular architectures in the solid state by direct hydrogen bonding interactions between fragments, in which a second component with a complementary functional group may be linked to N−H moieties to yield unique supramolecular systems via hydrogen bonds (type H).[30] In particular, the B linkage mode can be further connected to another metal ion by type C linkage mode. A survey of the Cambridge structural database (CSD)[31] revealed that only four complexes have this coordination mode.[32] Two of them are oligomers, and the other two are polymers with interesting magnetic properties.[32a,32d] Notably, there is no nickel or cobalt complex of Hbiim$^-$ in type C linkage mode reported so far. The biim^{2-} ligand forms polynuclear[34] and dinuclear[33] complexes which exhibit type D and type E coordination modes, respectively.

Considering the fact that the H_2biim ligand can exhibit various coordination modes, its complexes may further assemble into a higher dimensional structure via hydrogen bonds or metal−ligand interactions. We report herein the

(23) Hester, C. A.; Collier, H. L.; Baughman, R. G. *Polyhedron* **1996**, *15*, 4255.
(24) (a) Cancela, J.; Garmendia, M J. G.; Quiros, M. *Inorg. Chim. Acta* **2001**, *313*, 156. (b) Sang, R.; Zhu, M.; Yang, P. *Acta Crystallogr., Sect. E* **2002**, *58*, m172.
(25) Drew, M. G. B.; Felix, V.; Goncalves, I. S.; Kuhn, F. E.; Lopes, A. D.; Romao, C. C. *Polyhedron* **1998**, *17*, 1091.
(26) (a) Belanger, S.; Beauchamp, A. L. *Acta Crystallogr., Sect. C* **1999**, *55*, 517. (b) Fortin, S.; Beauchamp, A. L. *Inorg. Chem.* **2000**, *39*, 4886. (c) Fortin, S.; Fabre, P.-L.; Dartiguenave, M.; Beauchamp, A. L. *J. Chem. Soc., Dalton Trans.* **2001**, 3520.
(27) Maiboroda, A.; Rheinwald, G.; Lang, H. *Eur. J. Inorg. Chem.* **2001**, 2263.
(28) Etter, M. C. *Acc. Chem. Res.* **1990**, *23*, 120.
(29) (a) Ye, B.-H.; Xue, F.; Xue, G.-Q.; Ji, L.-N.; Mak, T. C. W. *Polyhedron* **1999**, *18*, 1785. (b) Fortin, S.; Beauchamp, A. L. *Inorg. Chem.* **2001**, *40*, 105. (c) Rau, S.; Böttcher, L.; Schebesta, S.; Stollenz, M.; Görls, H.; Walther, D. *Eur. J. Inorg. Chem.* **2002**, 2800. (d) Atencio, R.; Chacon, M.; Gonzalez, T.; Briceno, A.; Agrifoglio, G.; Sierraalta, A. *Dalton Trans.* **2004**, 505. (e) Ye, B.-H.; Ding, B.-B.; Weng, Y.-Q.; Chen, X.-M. *Inorg. Chem.* **2004**, *43*, 6866. (f) Larsson, K.; Öhrström, L. *CrystEngComm* **2004**, *6*, 354. (g) Ye, B.-H.; Ding, B.-B.; Weng, Y.-Q.; Chen, X.-M. *Cryst. Growth Des.* **2005**, *5*, 801.
(30) (a) Tadokoro, M.; Isobe, K.; Uekusa, H.; Ohashi, Y.; Toyoda, J.; Tashiro, K.; Nakasuji, K. *Angew. Chem., Int. Ed.* **1999**, *38*, 95. (b) Tadokoro, M.; Nakasuji, K. *Coord. Chem. Rev.* **2000**, *98*, 205. (c) Tadokoro, M.; Shiomi, T.; Isobe, K.; Nakasuji, K. *Inorg. Chem.* **2001**, *40*, 5476. (d) Tadokoro, M.; Kanno, H.; Kitajima, T.; Shimada-Umemoto, H.; Nakanishi, N.; Isobe, K.; Nakasuji, K. *Proc. Nat. Acad. Sci. U.S.A.* **2002**, *99*, 4950. (e) Öhrström, L.; Larsson, K.; Borg, B.; Norberg, S. T. *Chem.—Eur. J.* **2001**, *7*, 4805. (f) Benkstein, K. D.; Stern, C. L.; Splan, K. E.; Johnson, R. C.; Walters, K. A.; Venhelmont, F. W. M.; Hupp, J. T. *Eur. J. Inorg. Chem.* **2002**, 2818.
(31) *Cambridge structural database*, version 5.26; CCDC: Cambridge, Nov. 2004.
(32) (a) Martinez-Lorente, M. A.; Daham, F.; Sanakis, Y.; Petrouleas, V.; Bousseksou, A.; Tuchagues, J.-P. *Inorg. Chem.* **1995**, *34*, 5346. (b) Mayboroda, A.; Comba, P.; Pritzkow, H.; Rheinwald, G.; Lang, H.; van Koten, G. *Eur. J. Inorg. Chem.* **2003**, 1703. (c) Comba, P.; Mayboroda, A.; Pritzkow, H. *Eur. J. Inorg. Chem.* **2003**, 3042. (d) Galán-Mascarós J. R.; Dunbar, K. R. *Angew. Chem., Int. Ed.* **2003**, *42*, 2289.
(33) (a) Kaiser, S. W.; Saillant, R. B.; Butler, W. M.; Rasmussen, P. G. *Inorg. Chem.* **1976**, *15*, 2681. (b) Haddad, M. S.; Duesler, E. N.; Hendrickson, D. N. *Inorg. Chem.* **1979**, *18*, 141. (c) Garcia, M. P.; Lopez, A. M.; Esteruelas, M. A.; Lahoz, F. J.; Oro, L. A. *Chem. Commun.* **1988**, 793. (d) Garcia, M. P.; Lopez, A. M.; Esteruelas, M. A.; Lahoz, F. J.; Oro, L. A. *J. Chem. Soc., Dalton Trans.* **1990**, 3465. (e) Esteruelas, M. A.; Lahoz, F. J.; Lopez, A. M.; Onate, E.; Oro, L. A.; Ruiz, N.; Sola, E.; Tolosa, J. I. *Inorg. Chem.* **1996**, *35*, 7811. (f) de Souza Lemos, S.; Bessler, K. E.; Schulz Lang, E. *Z. Anorg. Allg. Chem.* **1998**, *624*, 30.(g) de Souza Lemos, S.; Bessler, K. E.; Schulz Lang, E. *Z. Anorg. Allg. Chem.* **1998**, *624*, 701. (h) Benkstein, K. D.; Hupp, T. J.; Stern, C. L. *Angew. Chem., Int. Ed.* **2000**, *39*, 2891. (i) Rau, S.; Ruben, M.; Buttner, T.; Temme, C.; Dautz, S.; Gorls, H.; Rudolph, M.; Walther, D.; Brodkorb, A.; Duati, M.; O'Connor, C.; Vos, J. G. *J. Chem. Soc., Dalton Trans.* **2000**, 3649. (j) Maiboroda, A.; Rheinwald, G.; Lang, H. *Inorg. Chem. Commun.* **2001**, *4*, 381. (k) Benkstein, K. D.; Stern, C. L.; Splan, K. E.; Johnson, R. C.; Walters, K. A.; Venhelmont, F. W. M.; Hupp, J. T. *Eur. J. Inorg. Chem.* **2002**, 2818.
(34) (a) Kaiser, S. W.; Saillant, R. B.; Butler, W. M.; Rasmussen, P. G. *Inorg. Chem.* **1976**, *15*, 2688. (b) Uson, R.; Gimeno, J.; Oro, L. A.; Martinez de Ilarduya, J. M.; Cabeza, J. A.; Tiripicchio, A.; Tiripicchio Camellini, M. *J. Chem. Soc., Dalton Trans.* **1983**, 1729. (c) Uson, R.; Oro, L. A.; Gimeno, J.; Ciriano, M. A.; Cabeza, J. A.; Tiripicchio, A.; Tiripicchio Camellini, M. *J. Chem. Soc., Dalton Trans.* **1983**, 323. (d) Oro, L. A.; Carmona, D.; Lamata, M. P.; Tiripicchio, A.; Lahoz, F. J. *J. Chem. Soc., Dalton Trans.* **1986**, 15. (e) Tzeng, B.-C.; Li, D.; Peng, S.-M.; Che, C.-M. *J. Chem. Soc., Dalton Trans.* **1993**, 2365. (f) Carmona, D.; Ferrer, J.; Mendoza, A.; Lahoz, F. J.; Oro, L. A.; Vigura, F.; Reyes, J. *Organometallics* **1995**, *14* (4), 2066. (g) Kircher, P.; Huttner, G.; Heinze, K.; Schiemenz, B.; Zsolnai, L.; Buchner, M.; Driess, A. *Eur. J. Inorg. Chem.* **1998**, 703. (h) Majumdar, P.; Peng, S.-M.; Goswami, S. *J. Chem. Soc., Dalton Trans.* **1998**, 1569. (i) Majumdar, P.; Kamar, K. K.; Castineiras, A.; Goswami, S. *Chem. Commun.* **2001**, 1292. (j) Kamar, K. K.; Falvello, L. R.; Fanwick, P. E.; Kim, J.; Goswami, S. *Dalton Trans.* **2004**, 1827.

syntheses, structural characterization, and magnetic and adsorbed properties of two new complexes $[M(H_2biim)_3]$-$[M(Hbiim)(btc)]\cdot 2H_2O$ (M = Co, (**1**); M = Ni, (**2**); btc = 1,3,5-benzenetricarboxylate), in which the $Hbiim^-$ ligand in the anionic $[M(Hbiim)(btc)]^{2-}$ moiety acts as a tridenate ligand (type C) connecting two adjacent metal ions into helical chains which are further bridged by the btc ligands into layers, whereas the $[M(H_2biim)_3]^{2+}$ cations act as pillars and link the anionic layers via robust hydrogen bonds resulting in pillared-layer microporous MOFs with one-dimensional (1D) channels. To the best of our knowledge, they are the first examples of hydrogen-bonded pillared-layer 3D networks constructed by the coordination complex cations.

Experimental Section

Materials and Methods. The reagents and solvents employed were commercially available and used as received without further purification. The C, H, and N microanalyses were carried out with a Vario EL elemental analyzer. The FT-IR spectra were recorded from KBr pellets in the range of 400−4000 cm^{-1} on a Bruker-EQUINOX 55 FT-IR spectrometer. ^1H NMR spectra were recorded on a Varian 300 MHz spectrometer at 25 °C. Thermogravimetric (TG) data were collected on a Netzsch TG-209 analyzer in nitrogen at a heating rate of 10 °C min^{-1}. Powder X-ray diffraction patterns were recorded on a D/Max-2200 diffractometer with Cu Kα radiation (λ = 1.5409 Å) at a scanning rate of 2° min^{-1} with 2θ ranging from 5 to 50°. The samples used for magnetic measurement were checked, to be sure that they were phase pure, by X-ray diffraction. Magnetic susceptibility data of powder samples were collected in the temperature range of 2−300 K in an applied field of 1 T with the use of a Quantum Design MPMS7 SQUID magnetometer. The diamagnetic corrections were estimated from the Pascal's constants (-402.6×10^{-6} cm^3 mol^{-1} for **1** and -387.6×10^{-6} cm^3 mol^{-1} for **2**).[35] The effective magnetic moment was calculated from the following equation: $\mu_{eff} = 2.828(\chi_M T)^{1/2}$. BET gas sorption was carried out on an accelerated surface area and porosimetry system (ASAP 2010, Micromeritics Ltd.) at 77 K. The isotherm measurements for methanol and acetone solvents were carried out on an automatic gravimetric adsorption apparatus (IGA-003 series, HIDEN ISOCHEMA Ltd) at 298 K. A known weight (60−150 mg) of the as-synthesized sample was placed in the quartz tube, and the sample was dried under high vacuum at 398 K for 3 h to remove the solvated water molecules before subsequent measurements.

Synthesis of H_2biim. The H_2biim ligand was synthesized in accordance with the published procedure.[36] Yield, 32%. Anal. Calcd for $C_6H_6N_4$: C, 53.73; H, 4.48; N, 41.79. Found: C, 53.41; H, 4.24; N, 41.56. FT-IR data (cm^{-1}): 3143 (m), 3074 (m), 3001 (s), 2896 (s), 2806 (s), 1546 (s), 1436 (m), 1405 (vs), 1333 (s), 1217 (m), 1105 (vs), 939 (s), 888 (m), 763 (m), 748 (s), 690 (m). ^1H NMR data (DMSO-d_6, ppm): 7.06 (C−H), 3.34 (N−H).

Syntheses of $[M(H_2biim)_3][M(Hbiim)(btc)]\cdot 2H_2O$ ($M = Co^{II}$, (1); $M = Ni^{II}$, (2)). $MCl_2\cdot 6H_2O$ (0.33 mmol; M = Co, Ni), H_2-biim (0.134 g, 1 mmol), and 2.67 mL of water were added to an aqueous solution (3.33 mL) containing sodium 1,3,5-benzenetricarboxylate (0.09 g, 0.33 mmol). The resulting mixture was adjusted to pH ≈ 5.8 with dilute hydrochloric acid. Orange and green crystalline products were collected, for **1** and **2**, respectively, after heating at 170 °C under hydrothermal conditions for 4 days. Yield, 10% for **1** and 30% for **2** based on metal salt. Anal. Calcd for $C_{33}H_{29}N_{16}O_8Co_2$ **1** (M_r = 896.59): C, 44.17; H, 3.23; N, 24.98. Found: C, 44.39; H, 3.44; N, 25.18. FT-IR (KBr, cm^{-1}): 3257−2519 (br), 1629 (m), 1609 (s), 1562 (s), 1528 (m), 1426 (s), 1366 (vs), 1315 (m), 1123 (m), 1101 (m), 751 (s), 715 (m), 692 (m). Anal. Calcd for $C_{33}H_{29}N_{16}O_8Ni_2$ **2** (M_r = 896.08): C, 44.17; H, 3.23; N, 24.98. Found: C, 44.53; H, 3.25; N, 25.28. FT-IR (KBr, cm^{-1}): 3148−2524 (br), 1631 (m), 1609 (s), 1561 (s), 1510 (m), 1426 (s), 1368 (vs), 1316 (m), 750 (s), 717 (m), 694 (m).

Table 1. Crystal and Structure Refinement Data for Complexes **1** and **2**

complex	**1**	**2**
molecular formula	$C_{33}H_{29}N_{16}O_8Co_2$	$C_{33}H_{29}N_{16}O_8Ni_2$
formula weight	896.59	896.08
crystal system	orthorhombic	orthorhombic
space group	*Ccc*2	*Ccc*2
a (Å)	18.1339(15)	17.6391(15)
b (Å)	39.530(4)	39.530(4)
c (Å)	11.6914(10)	11.7333(11)
V (Å^3)	8335.8(12)	8181.3(13)
Z	8	8
ρ_{calc} (g cm^{-3})	1.429	1.426
μ (mm^{-1})	0.863	0.985
reflections collected	25 705	21 907
independent reflections	8804	7418
data/restraints/parameters	7542/0/532	6128/0/532
R indices [$I > 2\sigma(I)$], wR2 (all data)[a]	0.0490, 0.1512	0.0539, 0.1264
$\Delta\rho_{max}/\Delta\rho_{min}$ (e Å^{-3})	0.89/−0.35	0.65/−0.38

[a] $R1 = \sum||F_o| - |F_c||/\sum|F_o|$, $wR2 = [\sum w(F_o^2 - F_c^2)^2/\sum w(F_o^2)^2]^{1/2}$.

X-ray Crystallography. Diffraction intensities for **1** and **2** were collected at 293 K on a Bruker Smart Apex CCD diffractometer with graphite-monochromated Mo Kα radiation (λ = 0.71073 Å). Absorption corrections were applied using SADABS.[37] The structures were solved by direct methods and refined with a full-matrix least-squares technique using the SHELXS-97 and SHELXL-97 programs, respectively.[38,39] Anisotropic thermal parameters were applied to all non-hydrogen atoms. The organic hydrogen atoms were generated geometrically (C−H 0.96 Å and N−H 0.86 Å). The hydrogen atoms of the water molecules were located from difference maps and refined with isotropic temperature factors. Analytical expressions of neutral-atom scattering factors were employed, and anomalous dispersion corrections were incorporated. In complex **2**, two water molecules were located from the electron density map, which were refined isotropically with site occupancy factors of 0.5. There may be one lattice water molecule that cannot be located from X-ray analysis (the TG and elemental analysis experiments show that there are two lattice water molecules in complex **2**). Crystal data as well as details of data collection and refinement for the complexes are summarized in Table 1. Selected bond distances and bond angles are listed in Table 2. The hydrogen bonding parameters are shown in Table 3.

Results and Discussion

Crystal Structures. Both **1** and **2** crystallize in the noncentrosymmetric space group *Ccc*2. The asymmetric unit consists of three components: a cation $[M(H_2biim)_3]^{2+}$, an anion $[M(Hbiim)(btc)]^{2-}$, and two lattice water molecules.

(35) Kahn, O. *Molecular Magnetism*; VCH: New York, 1993.
(36) Bernarducci, E. E.; Bharadwa, P. K.; Lalancette, R. A.; Krogh-Jes-Persen, K.; Potenza, J. A.; Schugar, H. J. *Inorg. Chem.* **1983**, *22*, 3911.
(37) Blessing, R. H. *Acta Crystallogr., Sect. A* **1995**, *51*, 33.
(38) Sheldrick, G. M. *SHELXS-97, Program for Crystal Structure Solution*; Göttingen University: Germany, 1997.
(39) Sheldrick, G. M. *SHELXL-97, Program for Crystal Structure Refinement*; Göttingen University: Germany, 1997.

Table 2. Selected Bond Lengths (Å) and Bond Angles (deg) of **1** and **2**[a]

	1	2		1	2
M(1)−N(1)	2.139(4)	2.092(5)	C(23)−C(24)	1.362(7)	1.371(7)
M(1)−N(3)	2.144(4)	2.102(4)	C(19)−N(14)	1.364(6)	1.375(7)
M(1)−N(5)	2.147(4)	2.105(4)	C(20)−N(13)	1.388(5)	1.388(6)
M(1)−N(7)	2.168(4)	2.118(4)	C(23)−N(15)	1.366(5)	1.362(6)
M(1)−N(9)	2.149(3)	2.117(4)	C(24)−N(16)	1.377(5)	1.365(6)
M(1)−N(11)	2.148(3)	2.110(4)	N(1)−M(1)−N(3)	78.7(1)	79.7(2)
M(2)−O(1)	1.998(2)	2.006(3)	N(5)−M(1)−N(7)	78.1(1)	79.6(2)
M(2)−N(13)	2.167(3)	2.112(4)	N(9)−M(1)−N(11)	78.3(1)	79.5(2)
M(2)−N(15)	2.030(4)	2.034(4)	O(1)−M(2)−N(13)	111.9(1)	108.7(1)
M(2)−O(5b)	2.131(2)	2.057(3)	O(1)−M(2)−N(15)	102.4(1)	98.3(1)
M(2)−N(16a)	2.039(3)	2.023(4)	O(1)−M(2)−O(5b)	81.8(1)	82.4(1)
C(31)−O(1)	1.252(4)	1.262(4)	N(13)−M(2)−N(15)	78.9(1)	79.6(2)
C(31)−O(2)	1.228(4)	1.232(5)	O(5b)−M(2)−N(13)	162.5(1)	164.7(2)
C(32)−O(3)	1.238(5)	1.254(7)	O(5b)−M(2)−N(15)	87.8(1)	88.4(1)
C(32)−O(4)	1.251(6)	1.223(7)	N(13)−M(2)−N(16a)	91.9(1)	91.7(2)
C(33)−O(5)	1.245(4)	1.258(6)	N(15)−M(2)−N(16a)	149.7(1)	160.3(1)
C(33)−O(6)	1.260(4)	1.261(5)	O(1)−M(2)−N(16a)	107.8(1)	101.2(1)
C(21)−N(13)	1.314(5)	1.316(7)	O(5b)−M(2)− N(16a)	94.1(1)	96.6(1)
C(21)−N(14)	1.347(5)	1.335(5)	O(1)−C(31)−O(2)	124.1(3)	123.6(4)
C(22)−N(15)	1.345(5)	1.334(7)	O(3)−C(32)−O(4)	125.1(4)	126.5(4)
C(22)−N(16)	1.325(6)	1.337(7)	O(5)−C(33)−O(6)	123.9(3)	123.4(4)
C(19)−C(20)	1.326(6)	1.356(8)			

[a] Symmetry code for **1**: (a) $-x, y, -^1/_2 + z$; (b) $^1/_2 - x, -^1/_2 - y, z$. For **2**: (a) $1 - x, y, -^1/_2 + z$; (b) $^1/_2 - x, -^1/_2 - y, z$.

Table 3. Hydrogen Bonding Parameters in **1** and **2**

D−H···A	D−H (Å)	H···A (Å)	D···A (Å)	D−H···A (deg)	symmetry operation for A
Complex **1**					
N(2)−H(2)···O(4)	0.86	1.87	2.696(3)	160	x, y, z
N(4)−H(4)···O(3)	0.86	1.86	2.718(3)	173	x, y, z
N(6)−H(6b)···O(2)	0.86	1.97	2.739(4)	148	$-x, -y, z$
N(8)−H(8b)···O(2)	0.86	1.94	2.716(3)	149	$-x, -y, z$
N(10)−H(10a)···O(6)	0.86	2.01	2.773(4)	148	$1 - x, -y, z$
N(12)−H(12b)···O(6)	0.86	1.92	2.698(3)	150	$1 - x, -y, z$
N(14)−H(14b)···O(1)	0.86	2.15	2.838(3)	137	$-x, y, -^1/_2 + z$
Complex **2**					
N(2)−H(2)···O(4)	0.86	1.84	2.682(3)	165	x, y, z
N(4)−H(4)···O(3)	0.86	1.85	2.695(4)	167	x, y, z
N(6)−H(6a)···O(2)	0.86	1.94	2.712(3)	149	$1 - x, -y, z$
N(8)−H(8b)···O(2)	0.86	1.99	2.752(3)	147	$1 - x, -y, z$
N(10)−H(10a)···O(6)	0.86	2.04	2.798(3)	146	$-x, -y, z$
N(12)−H(12b)···O(6)	0.86	1.90	2.681(3)	150	$-x, -y, z$
N(14)−H(14b)···O(1)	0.86	1.99	2.747(3)	147	$1 - x, y, ^1/_2 + z$

Each metal ion in $[M(Hbiim)(btc)]^{2-}$ is coordinated by three nitrogen atoms of two Hbiim's and two oxygen atoms of two carboxylate groups [M−O(1) = 1.998(2) and 2.006(3) Å, M−O(5b) = 2.131(2) and 2.057(3) Å for **1** and **2**, respectively], resulting in a distorted square pyramid structure [O(5b)−Co(2)−N(13) = 162.5(1)° and N(15)−Co(2)−N(16a) = 149.7(1)°, τ = 0.22, for **1** and O(5b)−Ni(2)−N(13) = 164.7(2)° and N(15)−Ni(2)−N(16a) = 160.3(1)°, τ = 0.07, for **2**], as shown in Figure 1. Each $Hbiim^-$ is simultaneously coordinated to one metal atom in a bidentate mode through the imino nitrogen atoms of both imidazole rings and in a monodentate type C linkage mode to another metal atom through the deprotonated amino nitrogen atom of the imidazolate ring, as shown in Scheme 1. A search of the CSD revealed only four complexes with this coordinate mode.[31] The complexes $Fe(Hbiim)_2$ (**3**) and $[Co_5(Hbbim)_6Cl_4(H_2O)_2]\cdot PhCH_3\cdot CH_3OH$ (**4**, where H_2bbim is 2,2′-bibenzimidazole) are three-dimensional (3D) and two-dimensional (2D) frameworks, respectively.[32a,32d] On the contrary, the osmium complexes $[Os(Hbiim)_2(OPPh_3)_2(PtL_1)](CF_3SO_3)_2(NO_3)\cdot 4H_2O$[32b] and $[Os(Hbiim)_2(OPPh_3)_2(RhClL_2)](NO_3)$[32c]

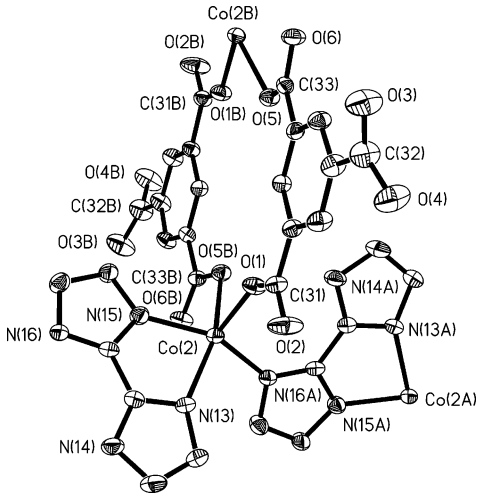

Figure 1. Coordination environment of Co(2) in the anion of **1**.

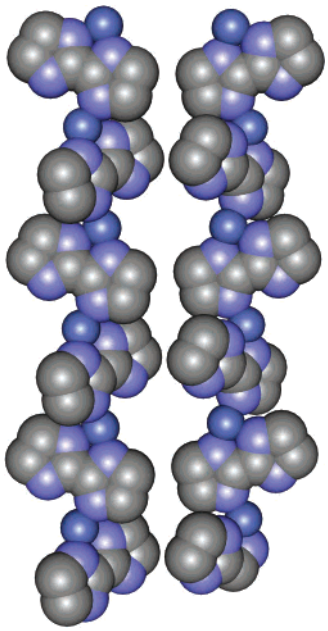

Figure 2. CPK drawing of the two helical structures in the anionic moiety of **1**.

(where L_1 = 2,6-bis(dimethylaminimethyl)phenyl and L_2 = cycloocta-1,5-diene) are trinuclear. The bond distances of the metal ion to the imidazole ring (M−N(13) = 2.167(3) Å for **1** and 2.112(4) Å for **2**) are longer than those of the metal ion to the imidazolate ring (M−N = 2.030(4) and 2.039(2) Å for **1** and 2.034(4) and 2.023(4) Å for **2**). This may be attributed to the facts that the nitrogen atoms of imidazole and imidazolate rings have different coordination abilities and the N(13) atom is located on the axial position. Interestingly, the bridging imidazolyl group connects the two adjacent metal ions into a helical chain along the *c*-axis, and these helices are alternately arranged in a left- and right-handed manner, as shown in Figure 2. The metal−metal distances along the *c*-axis are 5.969 and 5.964 Å for **1** and **2**, respectively, which are significantly shorter than those observed in **3** (6.248 Å)[32a] but longer than those in **4** (5.792 Å).[32d] Furthermore, each pair of helices is bridged by btc ligands with a distance of M(2)···M(2b) = 7.858(3) Å for **1**

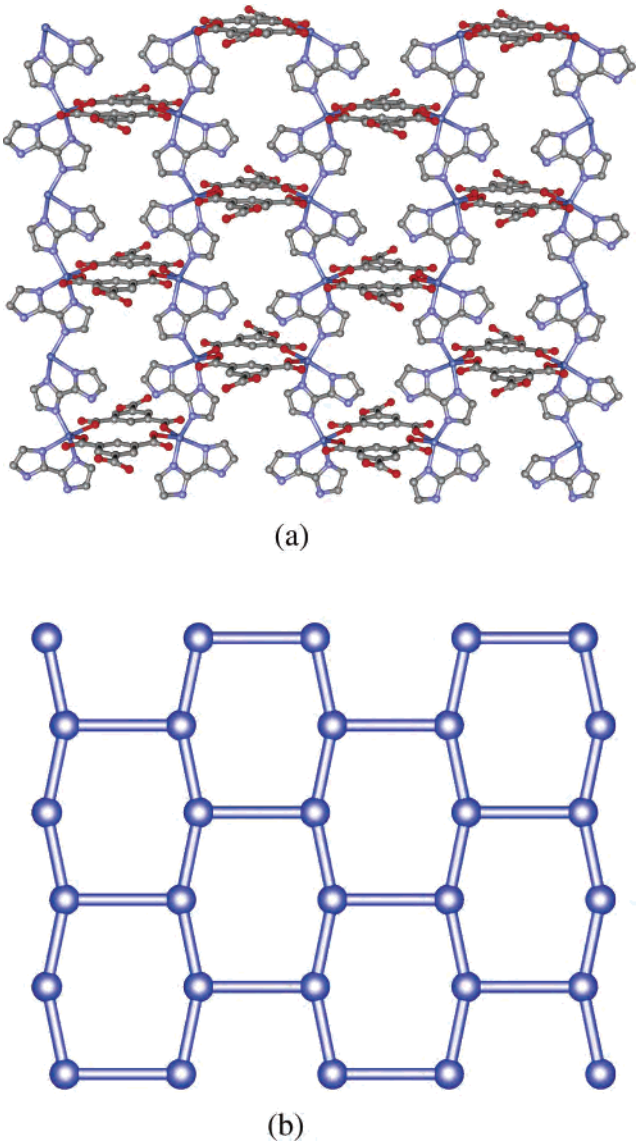

Figure 3. (a) Views of the 2D brick wall structure on the *ac* plane in the anionic layer of **1** and (b) its schematic diagram.

or 7.754(4) Å for **2** into an anionic brick wall-like structure parallel to the *ac* plane, as shown in Figure 3. Two carboxylate groups of each btc ligand are coordinated to metal ions in a monodendate fashion, and the remaining uncoordinated carboxylate group lies almost normal to the *ac* plane.

Each metal ion in $[M(H_2biim)_3]^{2+}$ is coordinated by the six nitrogen atoms of three H_2biim's (M−N = 2.139(4)−2.168(4) Å for **1** and 2.092(5)−2.118(4) Å for **2**), resulting in a distorted octahedral structure, as shown in Figure 4. Although the $[M(H_2biim)_3]^{n+}$ complexes were synthesized 40 years ago,[40] only three of these complexes have been characterized by X-ray single-crystal diffraction.[31] The metal−nitrogen distances observed herein are comparable with those observed in $[Fe(H_2biim)_3]CO_3$,[32a] $[Fe(H_2bbiim)_3]Cl_2$,[41] $[Ru(H_2biim)_3]Cl_2$,[42] $[Co(H_2biim)_3](NO_3)_3$,[30e] $[Cr(H_2biim)_2(Hbiim)]SO_4$,[43] $[Co(H_2bim)_3](ClO_4)_2$, and $[Fe(H_2bim)_3](ClO_4)_2$,[44] where H_2bim is 2,2′-bi-2-imidazolnyl. Moreover, the $[M(H_2biim)_3]^{2+}$ cations are embedded between the anionic $[M(Hbiim)(btc)]^{2-}$ layers and interlink two adjacent layers into a pillared-layer microporous MOF via robust N−H···O hydrogen bonds, as shown in Scheme 2 and Figures 5 and 6. The distances between the anionic layers are ca. 19.696 Å for **1** and 19.468 Å for **2**, respectively. It is noticeable that the dimensions of the channels are about 11.85 Å × 11.85 Å for **1** and 11.43 Å × 11.43 Å for **2** (defined by two central metal atoms in the channels). The lattice water molecules are stabilized in the channels by charge-assisted O−H···O hydrogen bonds [O(4)···O(8w) = 2.889(3) and 2.844(3) Å, O(3)···O(7w) = 2.813(3) and 2.791(4) Å for **1** and **2**, respectively]. Analysis of the crystal volume available for the solvents by using PLATON[45] shows that there are approximately 7.5% for **1** and 7.8% for **2**, but the volumes increase up to 16.4% for **1** and 16.0% for **2** after removal of the lattice water molecules. To the best of our knowledge, they are the first examples of the hydrogen-bonded pillared-layer 3D MOFs constructed by the coordination complex cations as pillars.

The most interesting observation is the supramolecular assembly between the $[M(H_2biim)_3]^{2+}$ cation and the $[M(Hbiim)(btc)]^{2-}$ anion via robustly heteromeric hydrogen-bonded synthons $R_2^2(9)$ and $R_2^1(7)$ (modes F and G of

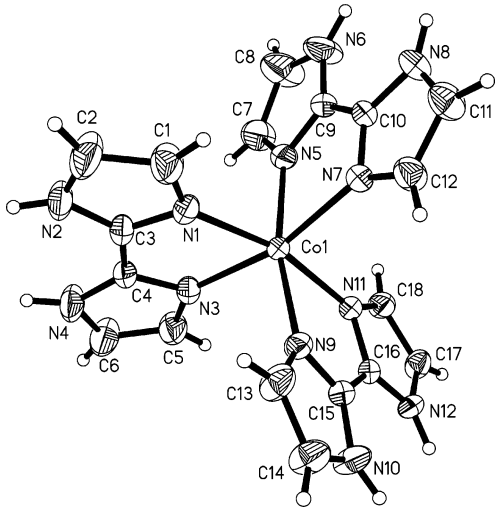

Figure 4. Coordination environment of Co(1) in the cation of **1**.

Scheme 2. Schematic Representation of the Pillared-Layer Microporous Metal−Organic Framework Constructed by the Cationic $[Co(H_2Biim)_3]^{2+}$ Pillars (Ball) and the Anionic $[Co(Hbiim)(btc)]^{2-}$ Layers (Rectangle) by Hydrogen Bonds and Electrostatic Interactions in **1**

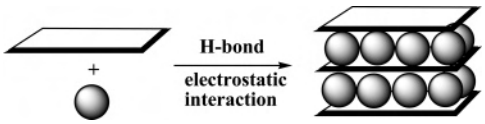

(40) (a) Holmes, F.; Jones, K. M.; Tomble, E. G. *J. Chem. Soc.* **1961**, 4790. (b) Abushamleh, A. S.; Goodwin, H. A. *Aust. J. Chem.* **1979**, *32*, 513.
(41) Boinnard, D.; Cassoux, P.; Petrouleas, V.; Savariault, J.-M.; Tuchagues, J.-P. *Inorg. Chem.* **1990**, *29*, 4114.
(42) Olmstead, M. M. Private communication, 1996.
(43) Larsson, K.; Öhrstrom, L. *CrystEngComm* **2003**, *5*, 222.
(44) (a) Roth, J. P.; Lovell, S.; Mayer, J. M. *J. Am. Chem. Soc.* **2000**, *122*, 5486. (b) Yoder, J. C.; Roth, J. P.; Gussenhoven, E. M.; Larsen, A. S.; Mayer, J. M. *J. Am. Chem. Soc.* **2003**, *125*, 2629.
(45) Spek, A. L. *Acta Crystallogr., Sect. A* **1990**, *46*, C34.

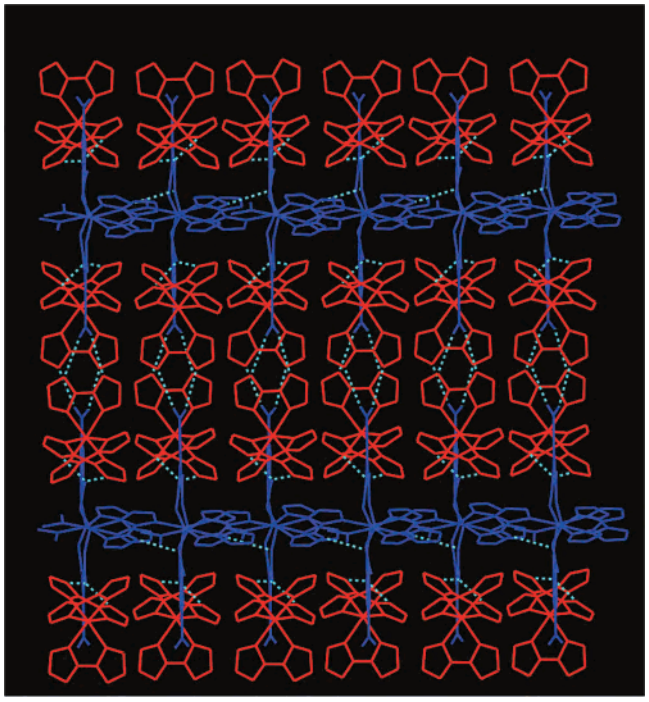

Figure 5. View of the pillared-layer 3D structure of **1** constructed by hydrogen bonds along the *a*-axis. The $[Co(H_2biim)_3]^{2+}$ ions as pillars are red, and the $[Co(Hbiim)(btc)]^{2-}$ layers are blue. All hydrogen atoms and water molecules are omitted for clarity.

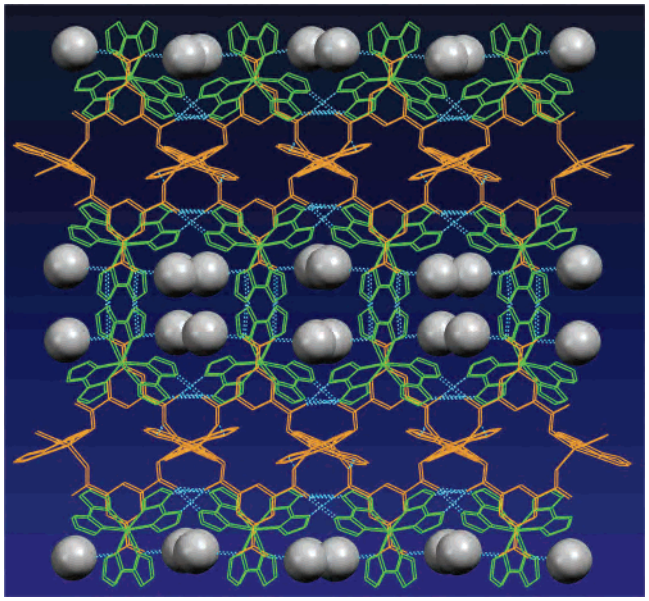

Figure 6. View of the microporous MOF constructed by hydrogen bonds with 1D channels along the *c*-axis in **1**. The cations $[Co(H_2biim)_3]^{2+}$ are green and the anions $[Co(Hbiim)(btc)]^{2-}$ orange, and lattice water molecules (gray balls) are located in the channels. All hydrogen atoms are omitted for clarity.

Scheme 1). Each $[M_2(btc)_2]^{2-}$ unit is connected with six homochiral Δ- or Λ-$[M(H_2biim)_3]^{2+}$ cations via a pair of $R_2^2(9)$ hydrogen-bonded synthons and two pairs of $R_2^1(7)$ hydrogen-bonded synthons to form a 2D layer lying parallel to the *ab* plane, as shown in Figure 7. Furthermore, the two optical isomers of Δ- and Λ-$[M(H_2biim)_3]^{2+}$ spontaneously separated and arranged alternately on the *ab* plane via hydrogen bonding. Therefore, the layers lying parallel to the

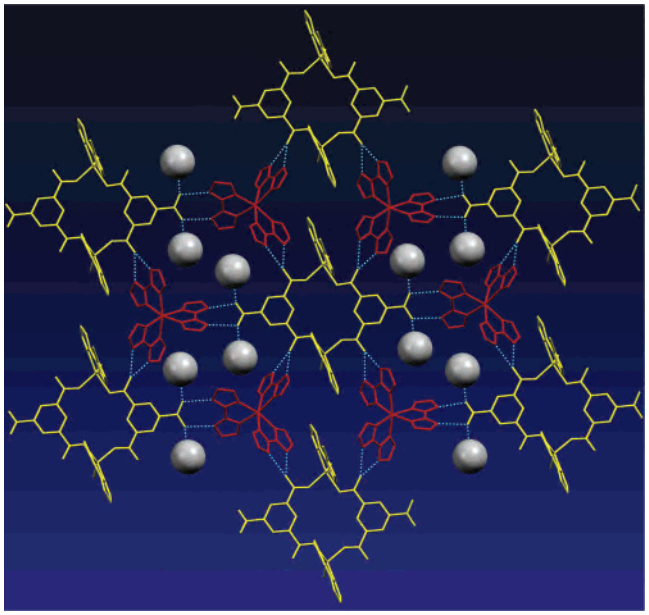

Figure 7. View of the X-ray crystal structure of **1** on the *ab* plane, showing a homochiral (Λ-$[Co(H_2biim)_3]^{2+}$) layer structure connected via hydrogen-bonded synthons. The gray balls are oxygen atoms of water molecules, and all hydrogen atoms are omitted for clarity.

ab plane are homochiral layers (Scheme 3). These homochiral layers are stacked alternately along the *c*-axis to give a heterochiral crystal packing.

Magnetic Properties. The magnetic susceptibility of **1** has been investigated in the temperature range of 2−320 K, and the plots of $\chi_M T$ and χ_M^{-1} vs T are shown in Figure 8. The $\chi_M T$ plot exhibits a continuous decrease upon cooling from ca. 5.92 $cm^3\ mol^{-1}$ K (6.88 μ_B) at 300 K to ca. 2.03 $cm^3\ mol^{-1}$ K (4.03 μ_B) at 2 K due to anti-ferromagnetic coupling. The temperature dependence of the magnetic susceptibility above 20 K obeys the Curie−Weiss law $\chi_M = C/(T - \theta)$. The $1/\chi_M$ vs T plot gives a Weiss constant of $\theta = -23.01$ K and a Curie constant of $C = 6.33\ cm^3\ mol^{-1}$ K, indicating a moderate anti-ferromagnetic coupling between the metallic centers along the helical chains or interactions between the chains and the cations. This value is slightly smaller than that observed in Co(II)-imidazolate (−26.2 to approximately −32.4 K).[7i] At room temperature, the $\chi_M T$ value is 5.92 $cm^3\ mol^{-1}$ K (6.88 μ_B), which is much higher than the calculated value [3.74 $cm^3\ mol^{-1}$ K (5.48 μ_B)] for the two isolated Co(II) ions ($S = {}^3/_2$ and $g = 2.0$), indicating that a significant orbital contribution is occurring. It is difficult to estimate the exchange interaction accurately within the Co(II) complexes because of the effect of spin−orbit coupling.[46]

The magnetic properties of **2** have also been studied, and the plots of $\chi_M T$ and χ_M^{-1} vs T are shown in Figure 9. The temperature dependence of the magnetic susceptibility obeys the Curie−Weiss law $\chi_M = C/(T - \theta)$ in the range of 2−300 K. The $1/\chi_M$ vs T plot gives a Weiss constant of $\theta = -3.64$ K and a Curie constant of $C = 2.46\ cm^3\ mol^{-1}$ K, corresponding to a *g*-value of 2.02, indicating a weak anti-

(46) Sun, B.-W.; Gao, S.; Ma, B.-Q.; Wang, Z.-M. *Inorg. Chem. Commun.* **2001**, *4*, 72.

Scheme 3. Schematic Representation of the (a) Λ-Homochiral and (b) Δ-Homochiral Layers Linked by Hydrogen Bonds in **1**

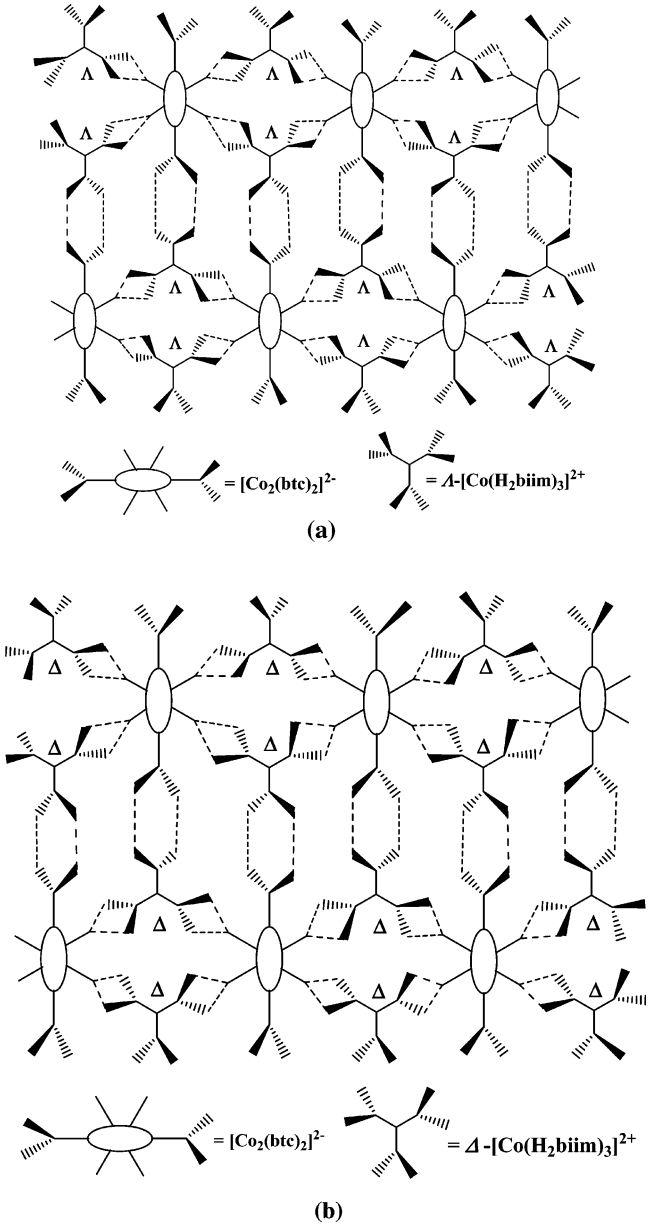

ferromagnetic coupling between the metallic centers along the helical chains, probably together with the weak antiferromagnetic coupling between chains and/or between cations and chains. The $\chi_M T$ value of 2.84 $cm^3\ mol^{-1}\ K$ (4.76 μ_B) at 300 K is slightly larger than the calculated value of 2.0 $cm^3\ mol^{-1}\ K$ (4.00 μ_B) for the two isolated Ni(II) ions ($S = 1$, $g = 2.0$). The magnetic properties of **2** are more complicated, as it contains a system of anionic layers interlinked by coordinate cations via hydrogen bonds. The magnetic exchange between the Ni(II) ions comes from two moieties, the coordination complex cations and the 2D coordination polymer. The former one should follow Curie behavior with $S = 1$, while the latter one can be regarded as chains due to the distance of Ni(II)···Ni(II) = 5.964 Å bridged by imidazolate along the chain being much shorter than that of 7.754 Å bridged by the btc ligand; also, the

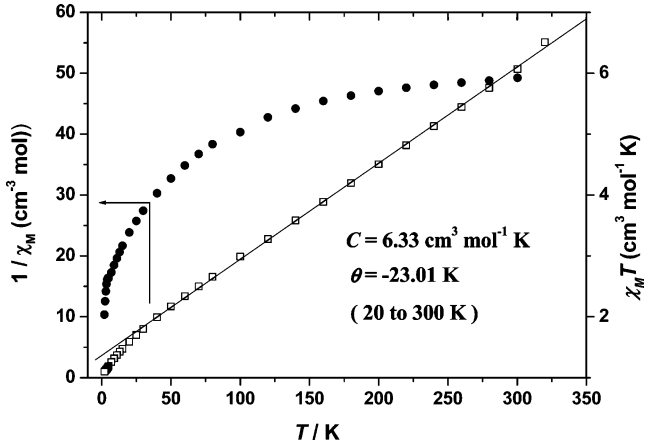

Figure 8. Temperature dependence of the $1/\chi_M$ and $\chi_M T$ product of **1**. The dots are experimental values, and the straight line represents the best fit.

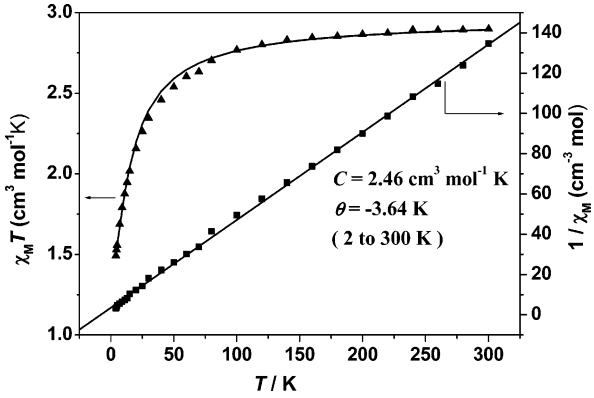

Figure 9. Temperature dependence of the $\chi_M T$ and $1/\chi_M$ product of **2**. The dots are experimental values, and the solid lines represent the best fits.

magnetic exchange through the bridging imidazolate should be much stronger than that through the btc ligand. Therefore, the magnetic susceptibility can be expressed by eq 1.

$$\chi_M = \chi_{cat} + \chi_{chain} \tag{1}$$

where

$$\chi_{cat} = \frac{N g_{cat}^2 B^2}{3kT} S(S+1)$$

The intrachain exchange interactions between isotropic Ni(II) centers, χ_{chain}, were analyzed with the Heisenberg infinite chain model which is given by eq 2.[35]

$$\chi_{chain} = \frac{2NB^2 g_{Ni}^2}{3kT} S(S+1) \frac{1+u}{1-u} \tag{2}$$

where $u = \coth[JS(S+1)/kT] - kT/JS(S+1)$, N is the Avogadro number, B is the Bohr magneton, k is the Boltzmann constant, and J is the intrachain coupling constant. Fitting of the experimental magnetic data by eq 2 gives unreasonable parameters. Taking into consideration the possibility of chain-to-chain and chain-to-cation interactions

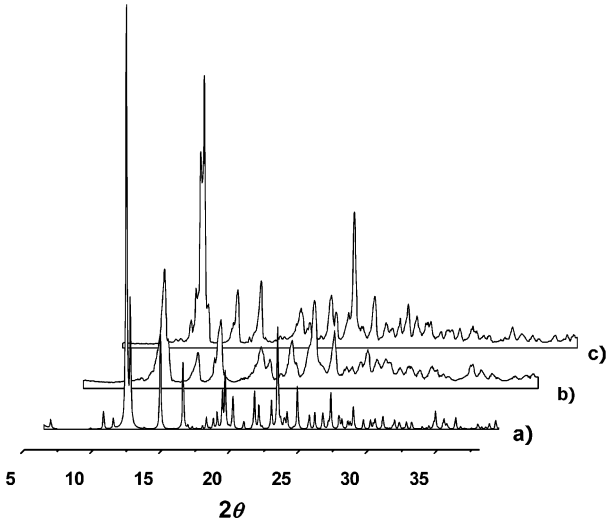

Figure 10. Powder XRD pattern of (a) a simulation based on the single-crystal analysis of **2**, (b) as-synthesized **2**, and (c) **2** after adsorption of methanol.

in the crystal lattice, the following correction for the molecular field is made:

$$\chi'_{\mathrm{M}} = \frac{\chi_{\mathrm{M}}}{1 - [\chi_{\mathrm{M}}(2zJ'/Ng_{\mathrm{Ni}}{}^2B^2)]} \qquad (3)$$

The best fitting of the experimental magnetic data by eq 3 gives the following parameters: $g_{\mathrm{cat}} = 2.296$, $g_{\mathrm{Ni}} = 2.564$, $J = -13.30\ \mathrm{cm}^{-1}$, $zJ' = -0.017\ \mathrm{cm}^{-1}$, and $R = 5.93 \times 10^{-5}$, where $R = \sum[(\chi_{\mathrm{M}}\ T)_{\mathrm{obs}} - (\chi_{\mathrm{M}}\ T)_{\mathrm{calcd}}]^2/\sum[(\chi_{\mathrm{M}}\ T)_{\mathrm{obs}}{}^2$. The results suggest that the interchain interactions are very weak compared with the intrachain interactions. In this fitting, the contribution from the zero field splitting of Ni(II) was ignored. This assumption may be true for the octahedral $[Ni(H_2biim)_3]^{2+}$ ion, but it is certainly not true for the five-coordinate Ni(II) ions in the anionic 2D layer. Nevertheless, the fitting results are satisfactory, as shown in Figure 9. The magnetic exchange in complex **2** is comparable to that in the known imidazolate-bridged Ni(II) complexes. For example, the interactions in **2** are stronger than those observed in the dinuclear complex $[Ni_2(tren)_2(biim)]^{2+}$ (tren = tris(2-aminoethyl)amine, $J = -2.9\ \mathrm{cm}^{-1}$)[47] and the cyclic tetranuclear complex $[Ni_4L_4]$ (L = *N*-salicylidene-*N*-(2-phenylimidazole-4-ylmethylidene)-1,3-propanediaminato, $J = -6.3\ \mathrm{cm}^{-1}$),[48] but they are weaker than those in another dinuclear complex, $[Ni_2(phen)_2(Im)]^{3+}$ (phen = 1,10-phenanthroline, Im = imidazole, $J = -30.4\ \mathrm{cm}^{-1}$).[8e]

Thermal Stability and Adsorption Property. The X-ray single-crystal structural analysis shows that the guest water molecules are anchored in open channels via the formation of hydrogen bonds with the carboxylate on the wall. The powder X-ray diffraction (XRD) of the as-synthesized product gives a satisfactory XRD pattern (Figure 10) which closely matches with the simulated one from the single-crystal data, indicating that such a pillared-layer microporous MOF constructed by hydrogen bonds is in a pure phase. Furthermore, thermal gravimetric analysis (TGA) and powder XRD measurements at different temperatures were performed to examine the robustness and thermal stability of the microporous framework upon removal of the guest molecules. The TGA experiments of the powder samples of **1** and **2** were carried out from 20 to 500 °C. The weight loss of 3.71% for **1** and 3.70% for **2** in the range of 20−120 °C (see Figures S1 and S2) corresponds to the loss of the guest water molecules (calculated 4.02%), indicating that the guest water molecules were completely removed at 120 °C. Figure 11 shows the XRD patterns of the as-synthesized sample of **2** at 100, 200, 300, 350, 400, and 450 °C. It is clear that the diffraction profiles below 350 °C are almost the same, indicating that the microporous framework is stable at this temperature and the crystal lattice remains intact after removal of the guest water molecules. The XRD pattern recorded at 400 °C exhibits a noticeable decrease in intensity, but all peaks still match with the simulated ones, suggesting that the porous framework is maintained. However, the sample became amorphous when the temperature was increased to 450 °C, as shown by the absence of diffraction peaks in the XRD pattern. Similar cases were also found in complex **1**.

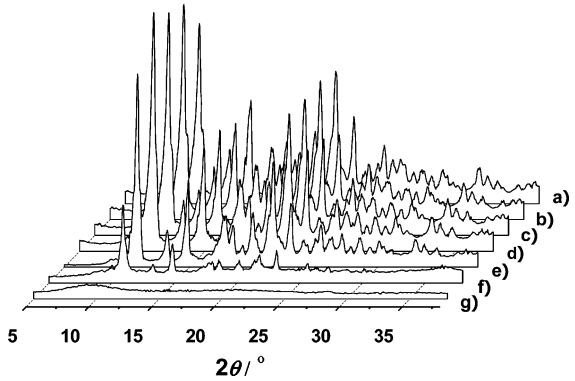

Figure 11. Powder XRD pattern of **2** at (a) 25 °C, (b) 100 °C, (c) 200 °C, (d) 300 °C, (e) 350 °C, (f) 400 °C, and (g) 450 °C.

The porosities and specific surface areas of the MOFs of **1** and **2** were estimated by measuring nitrogen gas sorption isotherms at 77 K. The adsorption isotherm of N_2 shows that only surface adsorption has occurred, indicating that nitrogen molecules cannot diffuse into the channels at this temperature. On the other hand, a methanol molecule was able to diffuse into the microporous MOF irreversibly at 298 K. The adsorption and deadsorption profiles are plotted in Figure 12, and the isotherms show an interesting hysteretic character. The amount of adsorption is calculated by Langmuir analysis, and it is found that ca. 1.03 and 1.01 methanol molecules can be adsorbed by each Co and Ni atom, respectively. The powder XRD pattern of the methanol-adsorbed sample matches closely with that of **2** (Figure 10), implying that there is no structural change in the pillared-layer microporous framework after adsorption of methanol. However, when acetone was used instead of methanol as an adsorbate, no

(47) Haddad, M. S.; Hendrichson, D. N. *Inorg. Chem.* **1978**, *17*, 2622.
(48) Mimura, M.; Matsuo, T.; Matsumoto, N.; Takamizawa, S.; Mori. W.; Re, N. *Bull. Chem. Soc. Jpn.* **1998**, *71*, 1831.

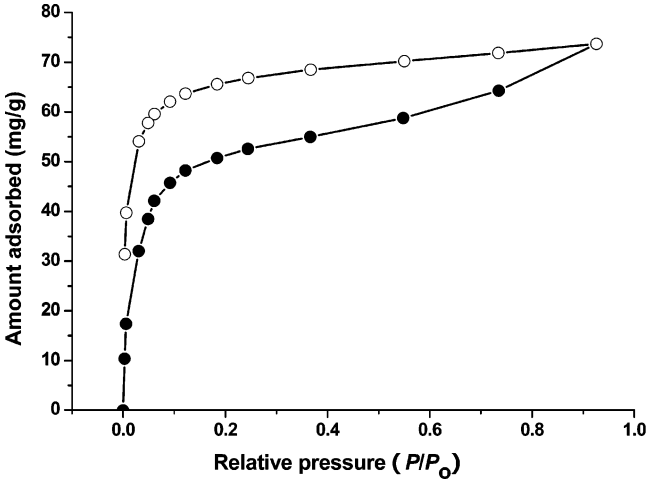

Figure 12. Methanol absorption (filled circles) and deabsorption (open circles) isotherms of **2** at 298 K.

adsorption behavior was found. This clearly shows that the microporous framework adsorbs methanol selectively, since the size of acetone molecule (26.8 $Å^2$) is larger than that of the methanol molecule (18.0 $Å^2$) and they are much larger than the size of the channels (diameter of 11.93 Å estimated by pore analysis).

Conclusion

We have synthesized two novel complexes $[M(H_2biim)_3]\cdot[M(btc)(Hbiim)]\cdot 2H_2O$ [M = Co, (**1**); M = Ni, (**2**)] under hydrothermal conditions. They consist of two distinct units: the monomeric cation $[M(H_2biim)_3]^{2+}$ and the 2D anionic polymer $[M(Hbiim)(btc)]^{2-}$. Interestingly, the $[M(H_2biim)_3]^{2+}$ cations act as pillars and interlink the anionic layers via robust heteromeric hydrogen-bonded synthons $R_2^2(9)$ and $R_2^1(7)$ to yield a pillared-layer microporous MOF with 1D channels. The microporous frameworks of **1** and **2** are stable up to 350 °C, and the guest water molecules in the channels can be removed without destroying the microporous framework. In addition, the microporous frameworks can selectively adsorb methanol molecules, suggesting a potentially useful application in molecular separation techniques.

Acknowledgment. This work was supported by the NSFC (Nos. 20371052 and 20131020) and the NSF of Guangdong (No. 031581).

Supporting Information Available: X-ray crystallographic file in CIF format for the structure determination of **1** and **2**, TG plots of complexes **1** and **2**, and plot of methanol adsorption and desorption isotherms of **1**. This material is available free of charge via the Internet at http://pubs.acs.org.

IC051195K